

Detection of Two-Phase Slug Flow Film Thickness by Ultrasonic Reflection

Lalu Febrina Wiranata¹, Narendra Kurnia Putra² and Dedy Kurniadi³

¹Engineering Physics, Institut Teknologi Bandung, Jawa Barat, Indonesia, ²Engineering Automation, Politeknik Negeri Bali, Bali, Indonesia.

ABSTRACT This study aims to detect and analyze slug flow film thickness in two-phase flow, providing detailed structural flow information. The ultrasonic or Doppler reflection method is employed to identify slug flow and detect detailed thickness. Additionally, electrical resistance tomography is used to image and confirm the presence of slug flow. A high-speed camera records the slug flow's shape in real-time, validating its existence. The ultrasonic reflection method offers high accuracy, with a measurement error rate of less than 1% based on experimental results. The study uses a homogeneous block calibration method to measure slug flow thickness. Graphical results reveal apparent differences between the slug flow regime, inner pipe wall, and outer pipe wall, with the first echo of slug flow being easily observable. The accuracy of results is attributed to the combination of field programmable gate array instruments and measurement methods, showcasing the study's novel approach. This research introduces a new perspective or novelty on slug flow in multiphase flow studies, highlighting an innovative method for detecting film thickness.

KEYWORDS

Slug flow film thickness
Ultrasonic reflection
Velocity flow
Electrical resistance tomography
Two-phase flow

INTRODUCTION

Slug flow is a common phenomenon in closed pipes, occurring in two-phase flow where liquid and gas phases mix, impacting the custody transfer or the efficiency of chemical reactions. Where, the slug flow pattern is a multiphase flow condition in a pipe system when the liquid phase and gas phase flow together in the form of slugs (bars or large oval bubbles), which are not homogeneous and can be accompanied by tiny bubbles. Usually slug flow occurs in piping systems that are arranged horizontally or vertically. To better understand the characteristics of slug flow conditions that often occur, several slug flow conditions are shown in (Falcone *et al.* 2010; Zhai *et al.* 2021), where slug flow can be categorized into several types of flow, namely plug, low-aerated, high-aerated to pseudo slug flow. This condition indicates that the slug combines flow rates with large and several tiny bubbles. The slug flow category is also shown in (Zhai *et al.* 2023), which maps the gas-liquid flow pattern in horizontal pipe conditions.

One of the main detrimental impacts of flow rate is increased pressure loss in a pipe or flow system. This is caused by the interaction between the liquid and gas phases, which produces turbulence in the flow. A slug moving faster than the average flow can cause a significant pressure drop in the system. Additionally, slug flow can impact the flow capacity of the system, where fluctuating flow velocities and changes in the flow profile can cause variations in the flow capacity acceptable to the system. In systems susceptible to slug flow, flow fluctuations can cause problems in unstable operations (Villarreal *et al.* 2006). This may affect system reliability and operational security. For example, in the oil and gas industry, slug flow can cause problems such as pipe erosion, vibration and risk of equipment failure (Al-Safran 2009).

There are also influences in phase separation applications, such as in oil and gas phase separators. Slug flow can also affect phase separation efficiency. This can result in a less effective phase mixture, requiring unique designs or controls to overcome this problem. To overcome the impact of slug flow, various control strategies, and technologies can be used, including better pipe design, the use of phase separators, the use of slug-dampening devices, and the use of advanced measurement technology. Understanding flow characteristics and slug flow modeling is also important to manage their impacts effectively. This is the primary motivation for developing a thickness of slug flow detection system, where the characteristics of slug flow must be understood to provide

Manuscript received: 29 August 2024,

Revised: 4 October 2024,

Accepted: 8 October 2024.

¹febrina.nata@gmail.com (Corresponding author).

²narend@itb.ac.id

³kurniadi@itb.ac.id

essential data for detecting flow transition patterns.

In the development of slug flow detection, Doppler ultrasonic technology was chosen for its ability to provide detailed and precise information about slug flow characteristics. Doppler can detect changes in the frequency of sound waves caused by the movement of slug flow within a fluid, enabling measurements of velocity, spatial distribution, and other characteristics of multiphase flows. Its advantages include compatibility with various fluid types, including gases and liquids, and the provision of high-resolution data. Consequently, the application of Doppler in this study enhances our understanding of flow properties and establishes a robust foundation for identifying gas-liquid flow regimes. Numerous academic references explore the flow characteristics related to Doppler signals. For example, [Nnabuife et al. \(2019\)](#) employed an ultrasonic Doppler sensor and a machine learning approach to predict gas-liquid flow regimes.

[Wang et al. \(2019\)](#) focused on detecting the spatial and temporal distribution of liquid velocity in horizontal gas-liquid flow, proposing a bubble flow identification method based on the maximum speed and maximum velocity difference ratio. Additionally, [Nnabuife et al. \(2020\)](#) utilized a deep artificial neural network to identify gas-liquid flow regimes in an S-shaped pipe, using features extracted from Doppler signals. [Weiling et al. \(2021\)](#) analyzed the Doppler spectrum via a continuous wave ultrasonic Doppler sensor, with some extracted statistical features being input into a multi-class SVM classification model to classify five oil-water flow patterns in horizontal pipes. Recent advancements have also been made in measuring velocity vector profiles using ultrasonic methods ([Hitomi et al. 2021](#); [Obayashi et al. 2008](#); [Tiwari and Murai 2021](#); [Zhang et al. 2022](#)). Furthermore, [Lin and Hanratty \(1987\)](#); [Shimomoto et al. \(2021\)](#) presents a method for detecting slug flow in gas-liquid mixtures using pressure sensors, which effectively distinguishes between slugs and pseudo-slugs.

The method's key strengths include a practical experimental approach and simple technology, achieving high detection rates for intermittent slug flow. However, it faces challenges such as scalability issues, complex data analysis, double detection in intermittent flows, and reduced accuracy for continuous slug flow in simulations. Overall, while Doppler ultrasonic technology provides significant advantages in detecting slug flow through its high-resolution data and versatility across various fluid types, it also encounters challenges, including the need for advanced algorithms for complex data interpretation, scalability concerns in larger systems, issues with double detection in intermittent flows, lower accuracy in continuous slug flows in real-time industrial applications.

This study presents a new perspective method for measuring film thickness in gas-liquid slug flow using an Ultrasonic Doppler or Ultrasonic Reflection (U_R) system, with the U_R method demonstrating superiority detail in detecting slug flow structures. In contrast to the research conducted by [Zhai et al. \(2021, 2023\)](#), which primarily showcased the cut-off signal form without providing detailed signal representations during slug flow or bubble detection, resulting in suboptimal numerical graph presentations, this research approach emphasizes a more comprehensive detailed analysis of slug flow thickness signal.

The technique employed is based on homogeneous calibration block measurements. This system utilizes a Field-Programmable Gate Array (FPGA) for data acquisition from the ultrasonic transducer. The FPGA offers a relatively high sampling rate of 64 MSPS (Mega-Samples Per Second) for each data loop process, allowing for detailed information retrieval from the ultrasonic transducer.

Additionally, we incorporate Electrical Resistance Tomography (ERT) as an imaging system to visualize the presence of two distinct phases in slug flow. For ERT, we employ an ARM-type microcontroller, which achieves a superior and more stable sampling rate compared to other types, delivering a sampling rate of 2.4 MSPS for each data collection session. The results indicate a commendable level of accuracy, with the U_R method effectively detecting the thickness of slug flow. Moreover, it was observed that the flow velocity, derived from the combination of ERT and U_R measurements, significantly influences the composition of slug flow, particularly its thickness.

In addition, the following parts of this article are organized as follows. Section 2 explains the primary ERT- U_R sensor's method, working principle, and corresponding to the detection slug flow film-thickness method. Section 3 is related to measurement systems and data acquisition, where the combination of FPGA instruments and measurement methods has great potential to be applied and is one of the novelty or new perspectives in this study. Apart from that, there is also an ERT system that functions as confirmation of the existence of different phases. Section 4 shows the results of the experimental verification and validation of the system used, where in this study, the first echo is very easy to observe. This can also be a problem-solving limitation, as detecting the first echo in the slug flow takes a lot of work. Therefore, measuring film thickness in a gas-liquid becomes easy to explore. Section 5 contains the conclusions of the study obtained.

MATERIAL AND METHODS

This section focuses on the basic concept of ultrasonic reflection or ultrasonic Doppler to collect surface (inner pipe wall) distance data to the ultrasonic transducer. Apart from that, f_d can also calculate the velocity of liquid and gas flow. The expected result that we want to know is the time of flight between the transmitter of ultrasonic waves and the time of receiver ultrasonic waves. However, in some situations, such as the presence of slug flow at the flow rate, it is challenging to find the desired information, thus the process of searching and identifying first echoes must be carefully observed. The next concept is the image reconstruction process using the ERT technique, and the main ERT aim is to identify essential differences between two different phases. However, of course, the ERT technique is not accurate enough to consistently determine the size and position of the slug flow, therefore in this study, ERT is only used to detect differences in images of the two objects and the average two-phase fluid velocity flow rate to ensure that it can support strengthening the presence of slugs in the fluid flow rate.

Principle of Ultrasonic Reflection or Ultrasonic Doppler

This section explains the basic concepts used to find ToF due to slug flow in the pipe cross-section. As seen in Figure 1, f_0 is the received frequency, f_d is the shift frequency, θ is a degree of transducer position in the pipe ([Falcone et al. 2010](#); [Zhang et al. 2022](#)). For the c_{water} value, it is 1497 m/s ([Bao et al. 2022](#)). Apart from that, there is also h , which is the position or depth of the echo pulse from the first echo detection in slug flow conditions, where Δt is the time difference between the transmitter and receiver, which can be stated that the value of f is proportional to the inverse of t .

$$f_d = f_r - f_0 = \frac{2U_R}{\cos \theta} f_0 \quad (1)$$

$$U_R = \frac{f_d c_{\text{water}}}{2f_0 \cos \theta} \quad (2)$$

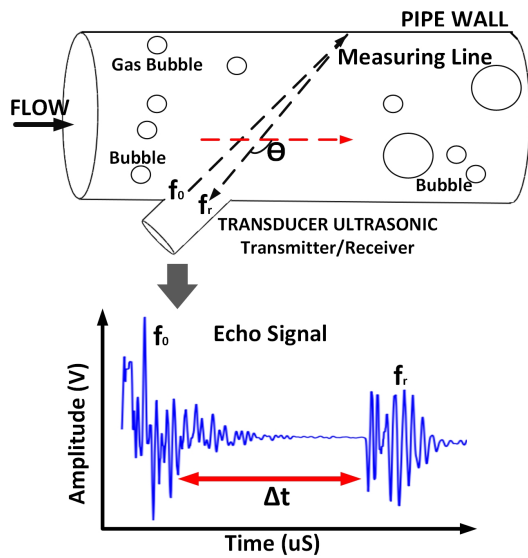


Figure 1 Principle of transducer ultrasonic reflection.

To find the average of flow velocity \bar{U}_R , Equation (3) is used, where A is the pipe cross-sectional area, R is the pipe radius, and y is the pipe diameter (Liu *et al.* 2018a).

$$\bar{U}_R = \frac{\int_0^{2R} U_R(y) \cdot 2\sqrt{y(2R-y)} dy}{A} \quad (3)$$

Meanwhile, to find the distance between the position of the transducer and the pipe, it is used Equation (4) (Zhai *et al.* 2021).

$$h = \frac{\Delta t \cdot c_{\text{water}}}{2} \quad (4)$$

Principle of Electrical Resistance Tomography Detection

Electrical resistance tomography (ERT) is an imaging technique that focuses on measuring the electrical resistance of an object or medium. The basic principle of this method is to measure the difference in resistance in a specific material or liquid, which has different characteristics from different resistance values. It can be done by exciting an AC electric current into the electrode to measure the characteristic value with a different electrode at another position. As shown in Figure 2, there are two ways to excite current into the vessel, and both of these methods are good for obtaining different signals from objects in the vessel. However, on this study, Figure 2(b) utilized opposite paired excitation because the electric current will generally pass through the container, allowing for the effective detection of the characteristics of non-uniform objects.

Opposite pair excitation method could be weak if the container is large enough. The distance between positive AC electric current and negative AC electric current will hamper the excitation current. In this study, the circle's diameter in the trial was relatively small, allowing the current to cross the object ideally. In other words, every method has its shortcomings and weaknesses. Therefore, it can be concluded that the advantage of the opposite pair method is that the sensitivity is quite good, provided that the distance between the sending and receiving electrodes is not too far, or it can be searched manually by moving objects on the vessel, where the graphic results will show a more sensitive response in any change in the movement of the object being measured.

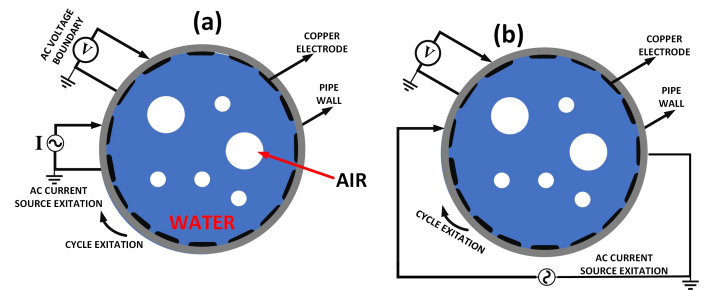


Figure 2 (a) adjacent pair excitation, (b) opposite pair excitation

Figure 3 explains the basic concept of ERT in reconstructing images, which initially come from several number value frames and then convert them into images with particular objects. For the first step, the AC electric current source is excited by rotating the 16 electrodes used, where the AC Boundary data takes the excitation data obtained 13 times with 16 measurements. Thus, we obtain 208 measurement limits for each resulting data frame. Next, the data is obtained to be used in the calculation values boundary. The data obtained is then searched for the potential distribution value with certain field boundaries, where the objective value is calculated and compared with the measurement data. If it is deemed to have met the appropriate threshold limit, then the image can be displayed. However, the iteration still needs to be increased. In that case, it is necessary to repeat the calculation of the resistance distribution values by carrying out updated calculations (conductivity updates) in the reconstruction equation (Liu *et al.* 2018b). In general, to solve the ERT problem, an approach using a forward problem is used (see Figure 3, finite element section), which aims to produce a mathematical model and can connect the distribution of resistance in the object with voltage measurements on the electrodes, where the model of the forward method in ERT is derived from the equation Maxwell which is written in Equation 5 (Liu *et al.* 2018b).

$$\nabla \cdot \sigma(x) \nabla u(x) = 0, \quad x \in \Omega \quad (5)$$

With value, $\nabla \cdot$ shows the divergence value, and ∇ is the gradient value, $\Omega \in \mathbb{R}^n$ is the data distribution in a specific domain (the region of interest). The conductivity value $\sigma(x)$ and electrical potential $u(x)$ depend on the domain where the x value is located. In simple terms, governing equations for the forward model can function to describe the relationship between the distribution of electrical resistance in an object and the measurement of voltage produced by electrodes placed around the object. Next, it is assumed that the current (I) is injected at the electrode with a specific domain boundary, which is written as $\partial\Omega$ in Equation (6) and Equation (7).

$$\int_{E_l} \sigma \frac{\partial u(x)}{\partial n} dS = I_l, \quad l = 1, 2, \dots, L \quad (6)$$

$$\sigma \frac{\partial u(x)}{\partial n} = 0, \quad \text{on } \partial\Omega \setminus \bigcup_{l=1}^L E_l \quad (7)$$

Equation (6) can be said to be the integral of the electrode with current flow (integral of current density), where E_l is the field at the l -th electrode, I_l is the current injected into E_l , L is the total number of electrodes, n is the outward normal vector, and dS is the surface of the element. Equation (7) is expressed as the equation for absence of current between one electrode and another, thus U_l

can be expressed as the l -th electrode potential, written in Equation (8).

$$u = U_l \text{ on } E_l, \quad l = 1, 2, \dots, L \quad (8)$$

However, in some cases, Equation (8) fails to calculate due to the double layer, as well as the high resistance contact between the electrode surface and the surface of specimen, which is the conductor in container. This concept in electrochemistry can prevent the transfer of electrical energy, which is modeled as the electrode resistance/impedance z_1 . As a result, Equation (9) is obtained (Demidenko *et al.* 2011):

$$u + z_1 \sigma \frac{\partial u(x)}{\partial n} = U_l \text{ on } E_l, \quad l = 1, 2, \dots, L \quad (9)$$

Finally, the charge conservation equation is expressed in Equation (10) and Equation (11) for the ERT potential (Somersalo *et al.* 1992):

$$\sum_{l=1}^L I_l = 0 \quad (10)$$

$$\sum_{l=1}^L U_l = 0 \quad (11)$$

Equation (10) and Equation (11) are chosen as the design equations of the ERT because each induced current corresponds closely to the magnitude and direction of the opposite sign, enabling Equation (10) and Equation (11) to calculate the average current value without being induced by the proximity of electrode pair.

The Gauss-Newton method in the ERT case is used to estimate the inverse non-linear value, with the main aim of minimizing the value of objective function $J(\sigma)$, written in Equation (12) (Ruan 2016):

$$J(\sigma) = \|U_{l,\text{meas}} - F(\sigma)\|_2^2 \quad (12)$$

where $U_{l,\text{meas}}$ is the potential electrical measurement vector value and F is the forward problem, which relates to the distribution vector of voltage values in an unknown area. The measured and calculated potential values are compared with the difference value (ε), written in Equation (13):

$$U_l = U_{l,\text{meas}} + \varepsilon \quad (13)$$

This is based on the frequent occurrence of ill-posed problems, which needs to be explicitly addressed using Tikhonov regularization (Graham 2007). To minimize the ERT function, it is necessary to add several basic conductivity constants (σ_0) as prior information or obtained from direct measurements. The resistance distribution calculation function can then be written as Equation (14), where λ is the hyperparameter value (Brinckerhoff 2018).

$$J_\lambda(\sigma_{k+1}) = \|U_{l,\text{meas}} - F(\sigma_k)\|_2^2 + \lambda \|\sigma_k - \sigma_0\|_2^2 \quad (14)$$

In addition, there is a parameter for updating the conductivity value, related to the conductivity update (σ_{k+1}), written in Equation (15):

$$\sigma_{k+1} = \sigma_k + \Delta\sigma \quad (15)$$

To calculate the value of $\Delta\sigma$, Equation (16) is used, which involves the Jacobian matrix calculation, discussed in more detail in (Brinckerhoff, 2018):

$$\Delta\sigma = (J^T J + \lambda^2 I)^{-1} J^T (U_{l,\text{meas}} - F(\sigma)) \quad (16)$$

MEASUREMENT SYSTEM

FPGA and ERT system

This section explains the primary system used to generate transmitter/receiver signals from ultrasonic waves, where the ultrasonic transducer type uses Sonatest with a central frequency of 10 MHz, which is embedded in the bottom wall of the pipe to ensure that it forms an angle of 90°. As seen in Figure 4, the pipe is attached to the wall, which aims to ensure that the transducer surface is in direct contact with two phases (liquid and air), thereby enabling maximum detection of the time of flight (ToF). This system uses a lattice iCE40HX4K FPGA type with 8Mb RAM. The working principle is that the FPGA sends high and low signals in a few microseconds to the MOSFET to open it to activate the DC-to-DC boost converter. Next, the boost converter or pulser generating the ultrasonic transducer generator will be active.

In the boost converter (NMT0572SC), there are 3 outputs 24 V, 48V, and 72 V, which have a low power consumption of 3W, and in the experiment, 48V was used to generate pulses from the ultrasonic transducer. The 48V voltage is sufficient to supply or generate the crystal in the transducer, and the amplitude can be adjusted under programming conditions using Python Code. Previously, the VHDL programming was communicated via FTDI is used to read the FPGA port, allowing the output to be directly converted into graphics.

The next step is data processing, carried out by the MCP4881, which is a component of time gain compensation (TGC), where TGC aims to compensate for the decrease in the amplitude of the ultrasonic signal, which occurs along with increasing depth when the signal propagates through different tissues or structures. The analog signal is then converted using the ADC100065 and processed briefly into a signal of a certain amplitude with a resulting sample rate of 128 MSPS each time the FPGA processes the data. The signal processed data is then sent via FTDI to USB, which in this case will be compensated into graphics. In this case, the ADC provides a 10-bit resolution, which is sufficient to analyze the output signal.

Figure 5(a) explains the configuration of the ERT system to detect the presence of slug flow or phase differences in closed flow pipes. The primary system used for control is an STM32 ARM microcontroller chip with a 32-bit Cortex CPU and 2.4 MSPS ADC, which provides a level of accuracy and precision that is reliable enough to execute DAC control, where the DAC is used to control mux/demux. In this case, an additional relay aims to separate the VCCS (voltage to control current) excitation because of the ability of the mux (multiplexer), which cannot pass AC current. The data is then received by the 12-bit RMS ADC by the demux (demultiplexer) in the form of different potential values for each electrode installed. It can be seen in Figure 5(b) that the composition form of the current excitation is colored blue while the potential difference receiver is colored green. For speed, the frequency used in executing the RMS ADC is activated at 108 MHz to ensure the data obtained can be executed quickly and accurately.

System configuration of flow measurement

Figure 6 explains the system configuration used, where the transducer is a Sonatest 10-MHz, the pipe has a diameter of 1.5 inches, a length of 2 meters, and a height of 1 meter. This system is embedded with a 3-unit detection system, namely ERT as the initial detection of two different phases, an ultrasonic transducer, and a high-speed camera with a resolution of 1080 × 2400 pixels and 960 frames per second, which aims to capture real-time images of the slug flow.

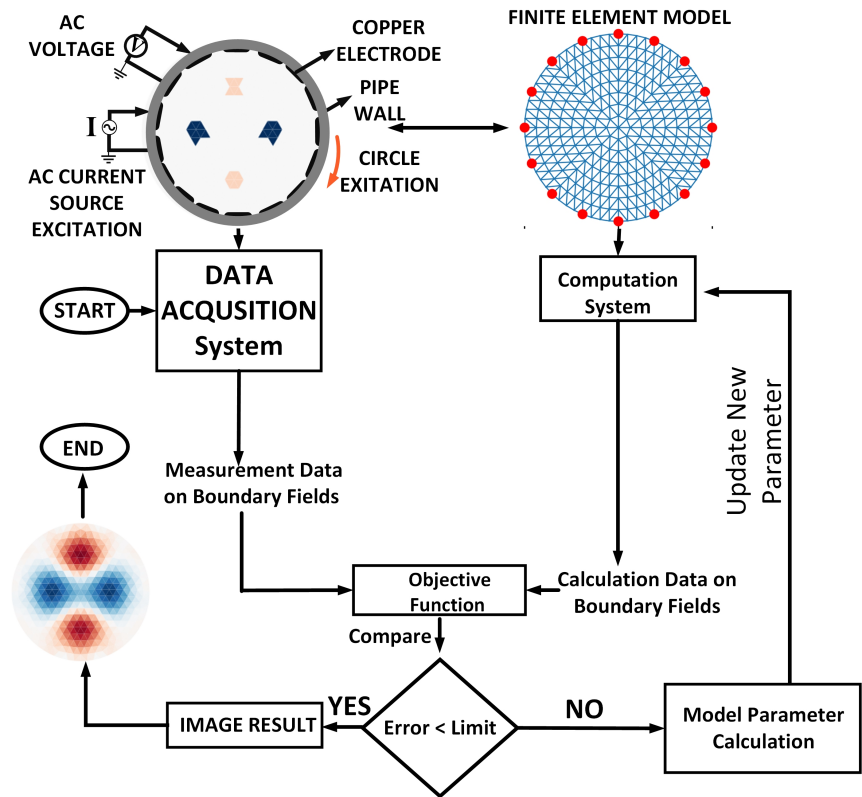


Figure 3 Data reconstruction image profile

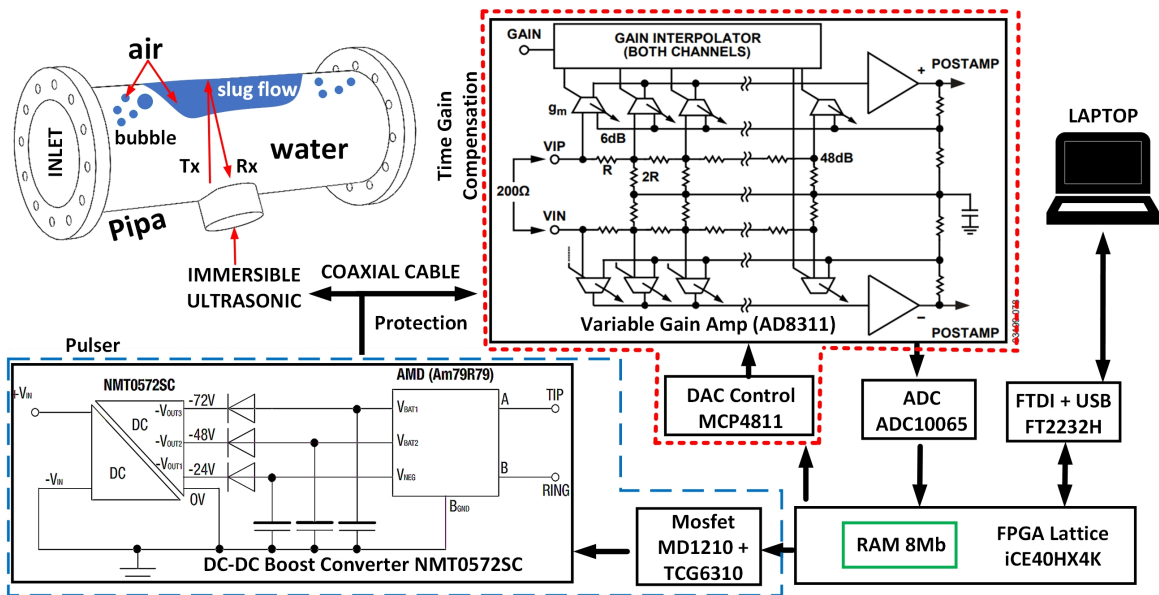


Figure 4 FPGA for ultrasonic reflection system.

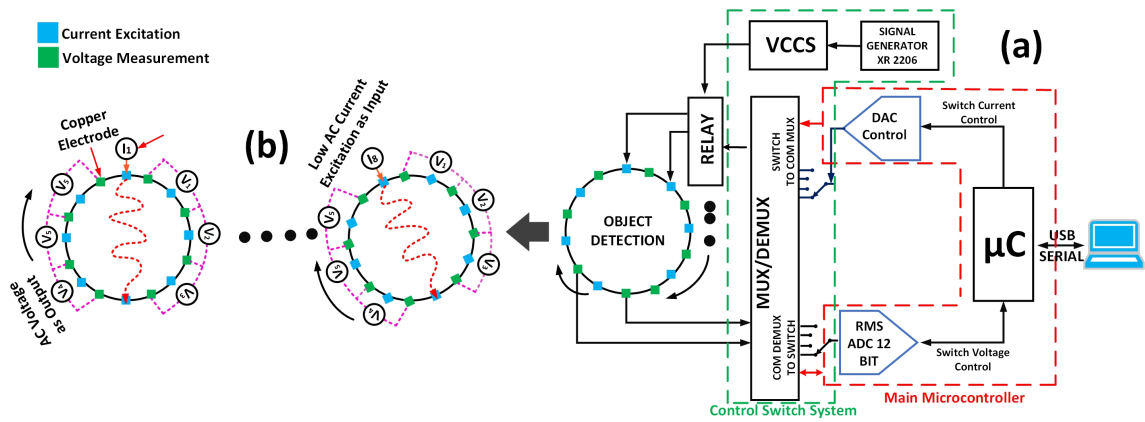


Figure 5 (a) ERT measurement system, (b) Measuring pipe tube (Wiranata et al., 2023).

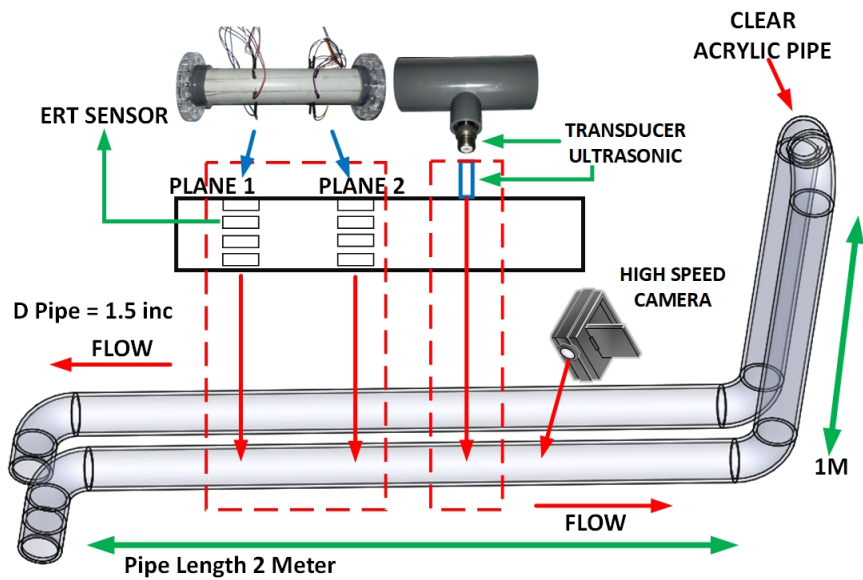


Figure 6 . Configuration System of Ultrasonic Reflection.

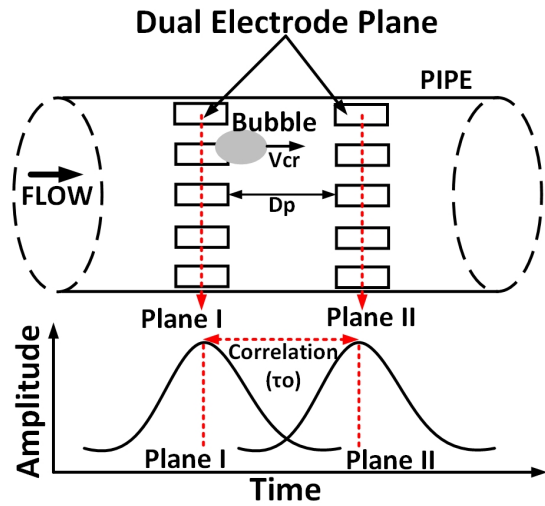


Figure 7 ERT dual plane.

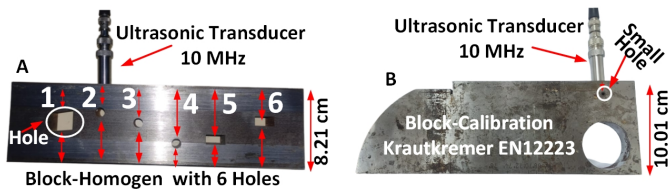


Figure 8 (a) Block homogen 6 holes, (b) Block calibration.

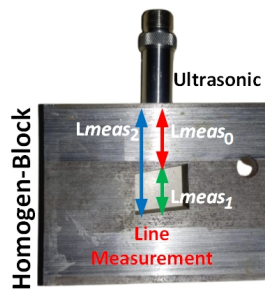


Figure 9 Block homogen measurement.

Table 1 Parameter measurement

Parameter	Values
Excitation Current AC	2 mA
Excitation Frequency	50 kHz
Electrode Number	8 Received & 8 Excitation
Data Speed Acquisition	10 frames/s
U_R	
Diameter Transducer	0.5 inch
Excitation Frequency	10 MHz
ADC Sampling Rate FPGA	64 MSPS
Excitation Voltage	48 V

Figure 7 explains how to obtain the velocity flow in a closed flow pipe using ERT, where D_p is the distance between planes I and II, and τ is the cross-sectional correlation between plane I and plane II. In Equation (18), $\overline{V_{CR}}$ is the average flow rate using dual ERT, with $V_{CR(n)}$ being the plane section (plane I or plane II).

$$V_{CR(n)} = \sum_{i,j} \frac{(V_{ij} - V_{ij0})}{V_{ij0}} \quad (17)$$

$$\overline{V_{CR}} = \lim_{T \rightarrow \infty} \left(\frac{1}{T} \int_0^T V_{CR1}(\lambda) V_{CR2}(\lambda + \tau) dt \right) \quad (18)$$

Placing the distance between plane I and plane II is very important for cross-correlation velocity measurement. If the distance is too far, the flow characteristics are challenging to detect, and one or two times the length of the pipe diameter is used (Deng et al. 2001). Table 1 explains several parameter values used in this research.

RESULT AND DISCUSSION

This section explains the results obtained from the experiment as a first step and as proof to find out the slug flow thickness and become a new perception in measuring the thickness of slug flow or become a novelty in this research, where the slug flow thickness measurement technique is adopted from the block homogeneous measurement process. The process starts from hollowing out a homogeneous block into 6 parts (see Figure 8(a)). Then, try measuring the width or thickness of the hole using ultrasonic waves transducer, as seen in Figure 8 technique used in the hole width search process. Meanwhile, the equation used refers to Equation (4) with c_{steel} 5920 m/s. The next step, namely looking for the presence of slug flow in the closed pipe cross-section, is the primary motivation for this research. Apart from that, there are also image results from photos using a high-speed camera to record the exact structure of the slug flow, and there are also imaging results from ERT as a comparison for detecting the presence of different particles in the slug flow.

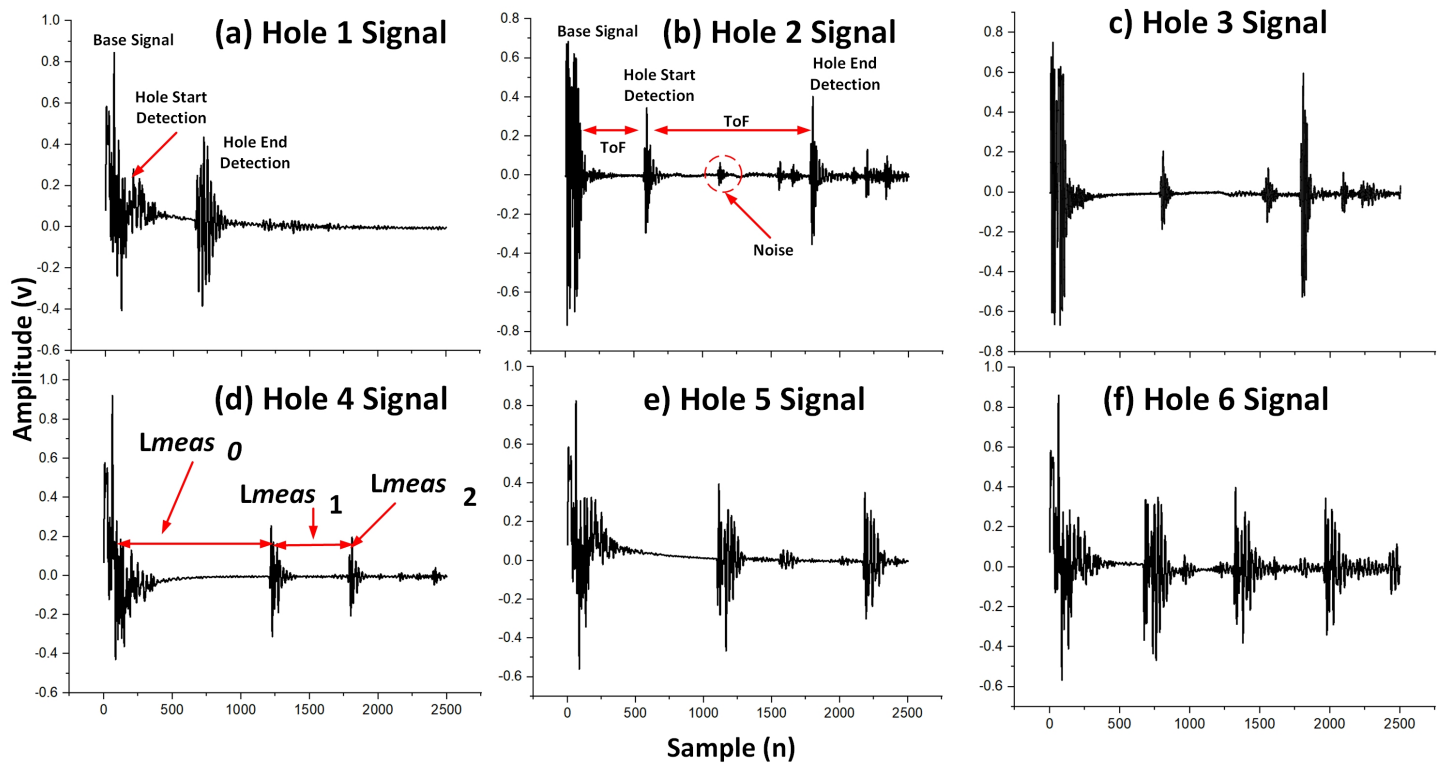


Figure 10 Percentage error between reference and measurement (a) 0.7346%. (b) 0.53066%. (c) 0.89116%. (d) 0.71103%. (e) 0.86957%. (f) 0.35891%.

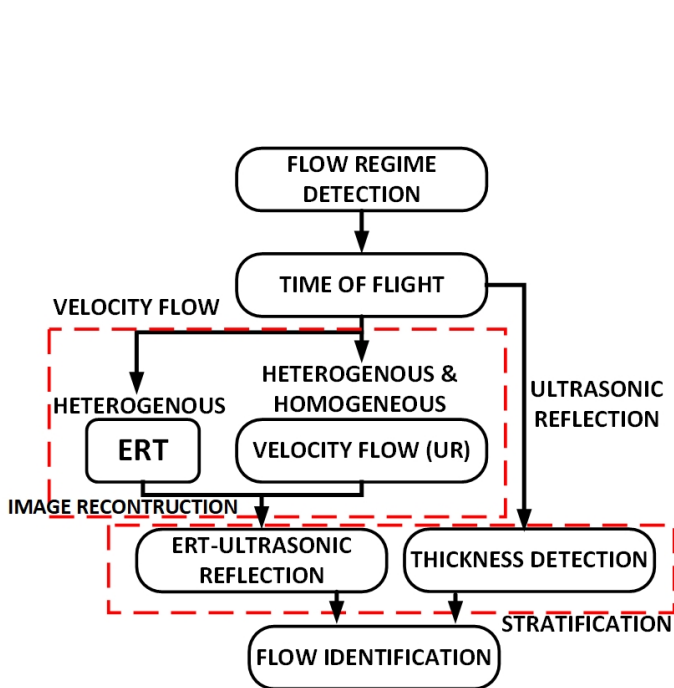


Figure 11 Flow regime identification.

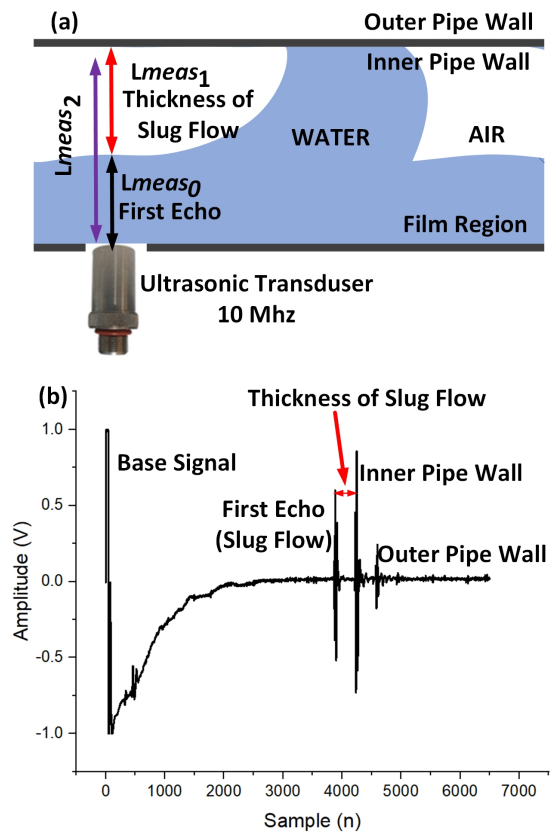


Figure 12 U_R Slug flow thickness detection and identification.

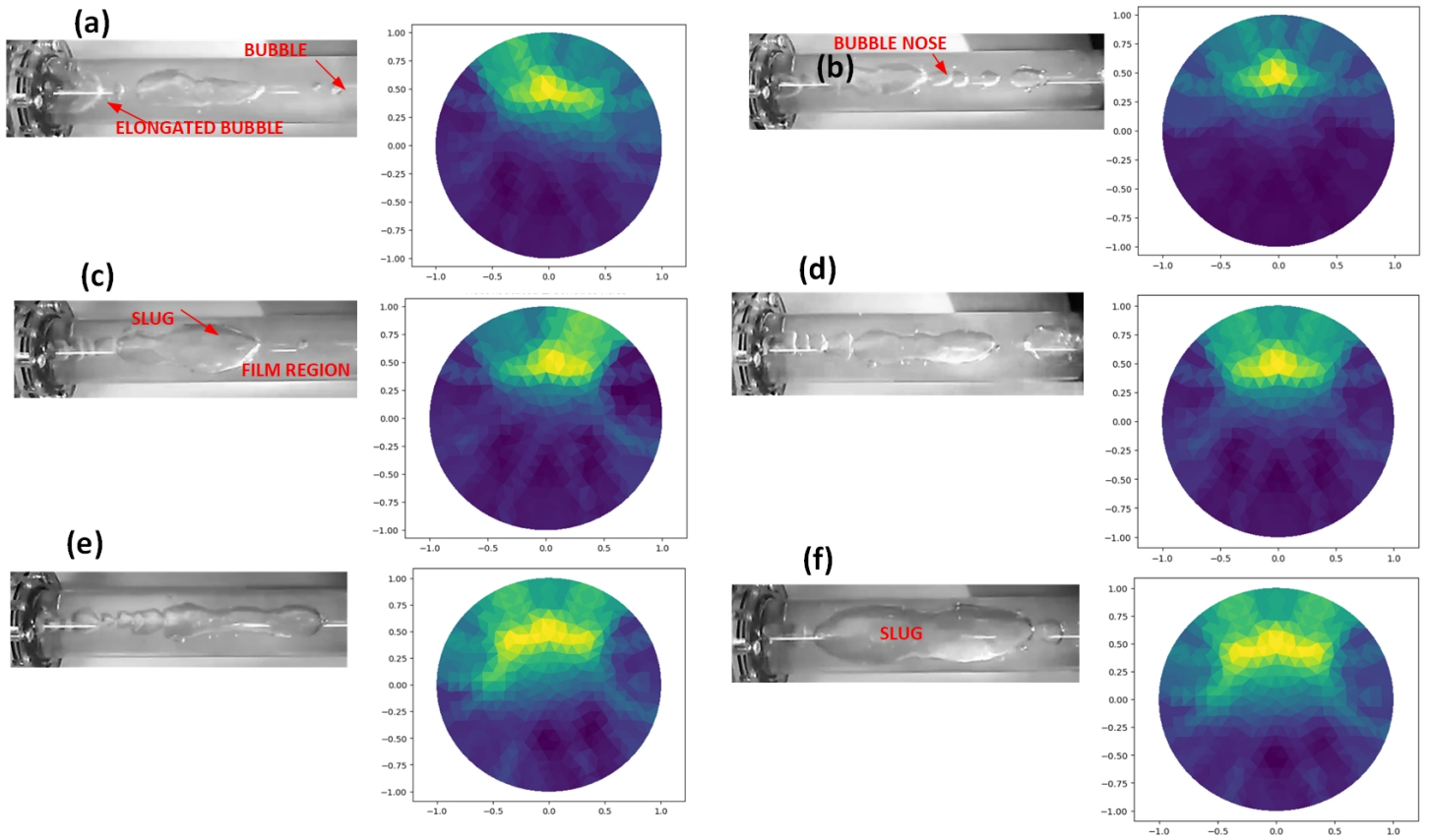


Figure 13 Velocity Flow (a) 0.73 m/s. (b) 0.76 m/s. (c) 0.95 m/s. (d) 0.98 m/s. (e) 1.18 m/s. (f) 1.2 m/s.

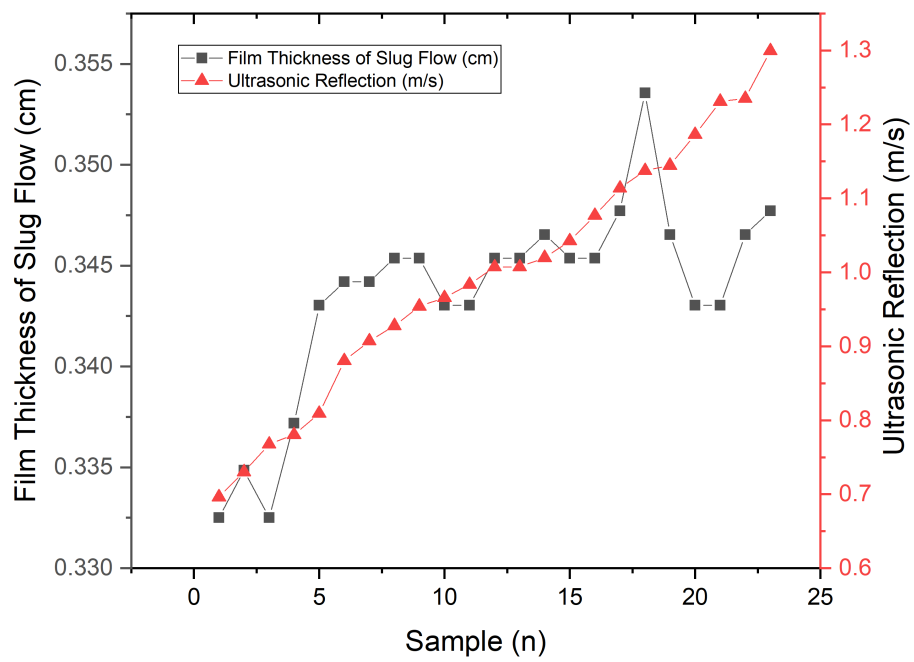


Figure 14 Film thickness of slug flow vs U_R Velocity Flow.

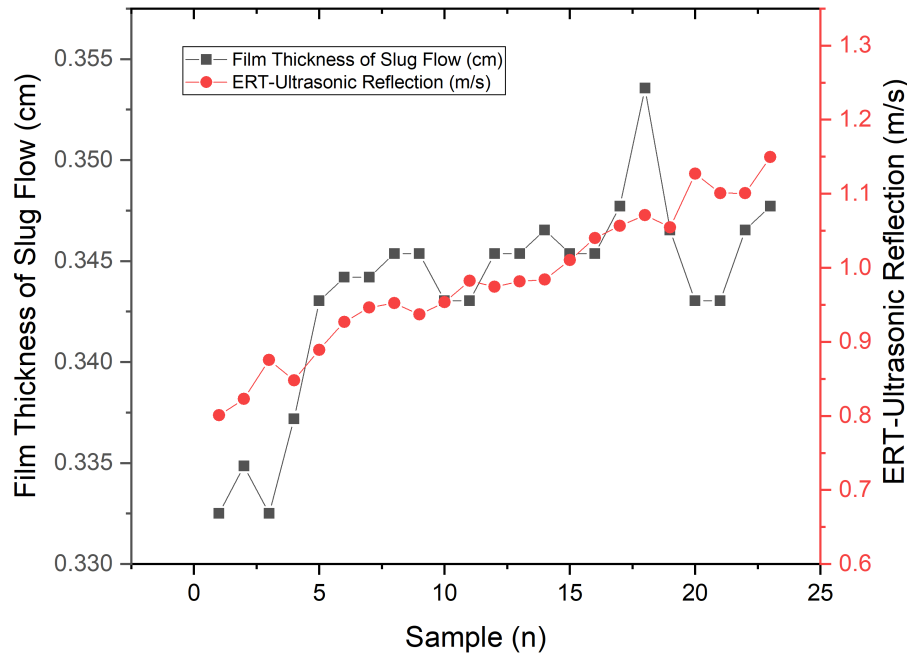


Figure 15 Film thickness of slug flow vs ERT- U_R Velocity Flow.

Validation method for measuring ultrasonic slug flow thickness

The use of homogeneous block calibration is a way to calibrate ultrasonic transducers to determine the level of error and accuracy produced by ultrasonic waves (ultrasonic transducers) to measure the thickness of objects using the ToF method, especially for the Sonatest immersible transducer type used. As seen in Figure 8. (b) The transducer is first tested on a homogeneous block calibration standard using Krautkremer EN12223. In the second step, the ultrasonic transducer was tested on a homogeneous block in which various holes were made at several points, the image of which is shown in Figure 8 (a), where the percentage error obtained by the measurement compared to the reference is no more than 1%.

To find the thickness from Figure 8(a), Equation (19) is used to determine the percentage error with Equation (20) when compared with the reference length in centimeters ($L_{ref_{meas}}$) which is the reference length from direct measurements using a digital clipper. Following Figure 9 is a detail of the measurement process.

$$L_{meas_1} = (L_{meas_2} - L_{meas_0}) - (L_{meas_2} - L_{ref_{meas}}) \tag{19}$$

$$\%Error = \frac{(L_{meas_1} - L_{ref_{meas_1}})}{L_{ref_{meas_1}}} \times 100 \tag{20}$$

Figure 10 is a graph of test results from U_R , where Figure 10 (a) to (f) represent the hole shape thickness in Figure 8(a) hole from 1 to 6. It can be seen in Figure 10 (d) and (e) that the error value is almost close to 1%. This occurs because the hole in the homogeneous block is quite far from the sensor, and there are other holes or measuring points close to other neighbor holes, which is the nature of the transducer ultrasonics have a spreading beam. Besides, the further the sound waves propagate, the bigger the beam. However, the results will be more reliable if the holes in

Figure 8 (a) are reversed when measuring the hole width. This occurs because other holes do not interfere with the measuring point.

Result of Slug Flow Thickness Detection

This section will explain the method or process of flow regime detection, where the essential information is obtained using the ToF method. As seen in Figure 11, ToF is the primary key to the information obtained, where the U_R method can detect heterogeneous and homogeneous presence from two different phases. At the same time, ERT is only able to detect heterogeneously. This is because ERT generally calculates the average flow velocity along the pipe cross-section. Meanwhile, calculating the thickness of slug flow using the ToF method can immediately be the primary reference. Thus, the final result obtained is in identifying and detecting slug flow thickness and flow rate in the pipe cross-section, which can be done using the U_R method or with ERT- U_R for a combination of speed and slug flow thickness.

Figure 12(a) explains the shape of the slug flow illustration in general, which often occurs in closed pipe cross-sections. That is then continued with Figure 12(b), which explains the process of identifying and determining the thickness of slug flow in pipe cross-sections. The difference between slug flow, inner pipe wall, and outer pipe wall is visible, as a result the measurements of the slug flow's thickness can be done quickly without looking for the threshold hold of the signal obtained. In general, to detect the thickness of the threshold slug flow, it takes time to identify it, especially if there is a lot of noise specifically. In several other studies, we have to look for the first echo or the location where the slug flow occurs, which takes longer compared to the concept in this study. This is the motivation and novelty of this research, namely information on the existence of slug flow, which is entirely

valid. This was obtained because the transducer used had a very high frequency, namely 10 MHz, which is rarely used to test the presence of slug flow in closed pipes. Apart from that, there is assistance from FPGA, which can process graphics significantly. In addition, the thickness of slug flow is difficult to identify in the first echo because there is phase mixing between water and air, making ToF characteristics challenging to observe. This, of course, requires accuracy to find the thickness of slug flow, but because of the accuracy of the transducer and FPGA from the system, the slug flow can be detected quite well, where the differences between each condition can be known. In addition, during the measurement process, not all flow conditions have slug flow because the characteristics of slug flow tend to change in pipe conditions that do not comply with standards. In this study, it was deliberately arranged to avoid following the rules for placing ultrasonic sensors, such as the conditions at $10xD$ and $5xD$ or other restrictions for placing sensors. This becomes a challenge due to conditions in the field, which cannot guarantee 100% laminar flow. However, if the flow is not symmetrical, it can still be detected well. Moreover, the graphic characteristics between the pipe wall and slug flow in ultrasonic transducers are very different, as seen in Figure 12, which is the characteristic shape of slug flow. In contrast, the specific characteristics of bubble flow will be explained in the following study.

Figure 13 explains the results of the combination of a high-speed camera and the imaging process using ERT seen in Figure 13 (a) – (f); there are variations in speed, where ERT is generally able to identify or detect the presence of two different phases with a yellow contrast light indicates high resistance while dark blue indicates low resistance. Or it can be stated that the bright yellow color contains the air fraction while the blue contains the water fraction, but due to spatial resolution problems, ERT is not good at imaging the shape of the slug flow in detail. Figure 13 also shows the forms of slug flow, which often occur in the trial dimension, to ensure that the general structure of slug flow can be depicted during the data collection process. If observed and compared with the reference, in this study, the form of slug flow observed was a low-aerated slug flow type, where the main profile contained a slug surrounded by a small amount of bubble flow.

Figure 14 explains the results obtained from the experiment between the number of sample film thickness of slug flow and the velocity flow results from U_R . It can be seen that the trend of the ultrasonic flowmeter is increasing because, in this case, the speed of water and air is increased slowly, where, in this case, the experiment can only be carried out by increasing both speeds simultaneously, aiming to see an increase in the same volume in each condition. In the beginning, the thickness of the film increased slightly even though it was found in a reasonably small range because the type of pipe had a diameter that was not too large. Then, it tends to stabilize at 0.345 cm. This proves that, in general, the slug flow thickness is difficult to know verifiable in the configurations tested in this research.

It can be seen in Figure 15 that the speed is slightly less linear between the addition of the flow rate and the process of measuring the flow rate using the ERT- U_R method. This is because ERT has a sensitivity that is not as good as U_R but has the potential to measure the average heterogeneous flow regime signal, where there is a slight pattern following the structure of the film thickness. This happens because the flow rate and void fraction of the fluid flow rate in heterogeneous conditions strongly influence slug flow. In detail, the concepts of fraction void and flow velocity will be presented in future research.

CONCLUSION

This study uses a combination of U_R and ERT methods to detect the presence of slug flow or two different phases, where the configuration uses a 1.5-inch diameter pipe. The concept of measuring the thickness of a homogeneous block is adopted in the U_R method to measure the thickness of slug flow. With the help of a transducer and FPGA, the location and thickness of the slug flow can be detected consistently. In addition, the U_R method can monitor the appearance of homogenous and heterogeneous differences in slug flow conditions, making this method optimal for use in two-phase states. Following are some summaries obtained:

- The slug flow measurement technique is adopted from the block-homogeneous measurement process with error less than 1%.
- It can be stated that the bright yellow color contains the water fraction while the blue water fraction is in the ERT results, but due to spatial resolution problems, ERT is not good at imaging in detail the shape of the slug flow
- A high-speed camera is used to record the shape of the slug flow through images definitively, and the results of the ERT imaging technique are used to compare and detect the presence of different particles in the slug flow.
- If observed and compared with the reference (Zhai *et al.* 2021), in this study, the form of slug flow observed is a low-aerated slug flow type, where the main profile contains a slug surrounded by a small distribution amount of bubble flow.
- From the results of the combination of the ERT- U_R method, it was found that ERT has a sensitivity that is not as good as U_R but has the potential to measure the average heterogeneous flow regime signal, where a slight pattern can be seen following the structure of the film thickness. This happens because the flow rate, velocity, and void fraction of the fluid flow rate in heterogeneous conditions strongly influence slug flow.
- A new approach is introduced to determine liquid film thickness by utilizing the instantaneous velocity profile. The liquid film thickness can be reliably measured by identifying the size of slug flow.
- The FPGA system developed is capable of delivering significant results due to the accuracy and reliability of the system's design.
- In general, the main results show that ERT is used to depict the fundamental structure of the velocity profile, while U_R is applied to measure the velocity and provide detailed measurements of the slug flow film thickness.

Finally, this study presents a new perspective method to detect multi-scale slug flow structures, where the speed and thickness of slug flow can influence each other or vice versa. Besides, seeing the consistency of slug flow can also be the basis for modelling and developing flow transition models. Moreover, the U_R method is the most suitable method for determining the thickness of slug flow. It is more economical because it only requires one type of transducer, making it very prospective for use in slug flow conditions. Additionally, by knowing the liquid film thickness of the slug, the void fraction development process better becomes where the composition of different phases can be learned such that it can be implemented across various industrial sectors, including the upstream oil and gas industry, pharmacy industry, freshwater distribution or freshwater management, metering systems, and custody transfer for volumetric systems.

Acknowledgments

This is work funded in part by Center Education Services (Pusat Layanan Pendidikan) Ministry of Education, Culture, Research and Technology of the Republic of Indonesia, and also LPDP under Basiswa Kemendibudristek Grant 202209091514.

Availability of data and material

The data collected in this study are available from the corresponding author upon reasonable request.

Conflicts of interest

The authors declare that there is no conflict of interest regarding the publication of this paper.

Ethical standard

The authors have no relevant financial or non-financial interests to disclose.

LITERATURE CITED

- Al-Safran, E., 2009 Investigation and prediction of slug frequency in gas/liquid horizontal pipe flow. *Journal of Petroleum Science and Engineering* **69**: 143–155.
- Bao, Y., C. Tan, and F. Dong, 2022 Oil–water two-phase flow volume fraction measurement based on nonlinear ultrasound technique. *IEEE Transactions on Instrumentation and Measurement* **71**: 1–9.
- Brinckerhoff, M., 2018 Comparison of electrical impedance tomography reconstruction algorithms with eiders reconstruction software.
- Demidenko, E., A. Borsic, Y. Wan, R. J. Halter, and A. Hartov, 2011 Statistical estimation of eit electrode contact impedance using a magic toeplitz matrix. *IEEE Transactions on Biomedical Engineering* **58**: 2194–2201.
- Deng, X., F. Dong, L. J. Xu, X. P. Liu, and L. A. Xu, 2001 The design of a dual-plane ert system for cross correlation measurement of bubbly gas/liquid pipe flow. *Measurement Science and Technology* **12**: 1024–1031.
- Falcone, G., G. F. Hewitt, and C. Alimonti, 2010 *Multiphase flow metering*. Elsevier.
- Graham, B. M., 2007 Enhancements in electrical impedance tomography (eit) image reconstruction for three-dimensional lung imaging.
- Hitomi, J., S. Nomura, Y. Murai, G. De Cesare, Y. Tasaka, *et al.*, 2021 Measurement of the inner structure of turbidity currents by ultrasound velocity profiling. *International Journal of Multiphase Flow* **136**: 103540.
- Lin, P. Y. and T. J. Hanratty, 1987 Detection of slug flow from pressure measurements. *International Journal of Multiphase Flow* **13**: 13–21.
- Liu, B., B. Yang, C. Xu, J. Xia, M. Dai, *et al.*, 2018a pyeit: A python based framework for electrical impedance tomography. *SoftwareX* **7**: 304–308.
- Liu, W., C. Tan, X. Dong, F. Dong, and Y. Murai, 2018b Dispersed oil–water two-phase flow measurement based on pulse-wave ultrasonic doppler coupled with electrical sensors. *IEEE Transactions on Instrumentation and Measurement* **67**: 2129–2142.
- Nnabuife, S., B. Kuang, J. Whidborne, and Z. Rana, 2020 Non-intrusive classification of gas-liquid flow regimes in an s-shaped pipeline riser using a doppler ultrasonic sensor and deep neural networks. *Chemical Engineering Journal* **403**: 126401.
- Nnabuife, S., K. E. Pilario, L. Lao, Y. Cao, and M. Shafiee, 2019 Identification of gas-liquid flow regimes using a non-intrusive doppler ultrasonic sensor and virtual flow regime maps. *Flow Measurement and Instrumentation* **68**.
- Obayashi, H., Y. Tasaka, S. Kon, and Y. Takeda, 2008 Velocity vector profile measurement using multiple ultrasonic transducers. *Flow Measurement and Instrumentation* **19**: 189–195.
- Ruan, T., 2016 Development of an automated impedance tomography system and its implementation in cementitious materials.
- Shimomoto, Y., K. Ikeda, H. Ogawa, Y. Nakatsu, and I. Yamamoto, 2021 Detection of slug flow generated in horizontal pipeline. *Sensors and Materials* **33**: 947.
- Somersalo, E., M. Cheney, and D. Isaacson, 1992 Existence and uniqueness for electrode models for electric current computed tomography. *SIAM Journal on Applied Mathematics* **52**: 1023–1040.
- Tiwari, N. and Y. Murai, 2021 Ultrasonic velocity profiler applied to explore viscosity–pressure fields and their coupling in inelastic shear-thinning vortex streets. *Experiments in Fluids* **62**: 185.
- Villarreal, J., D. Laverde, and C. Fuentes, 2006 Carbon-steel corrosion in multiphase slug flow and co2. *Corrosion Science* **48**: 2363–2379.
- Wang, S.-Q., K.-W. Xu, and H.-B. Kim, 2019 Slug flow identification using ultrasound doppler velocimetry. *International Journal of Heat and Mass Transfer* **148**: 119004.
- Weiling, L., C. Tan, and F. Dong, 2021 Doppler spectrum analysis and flow pattern identification of oil-water two-phase flow using dual-modality sensor. *Flow Measurement and Instrumentation* **77**: 101861.
- Zhai, L., H. Xia, H. Xie, and J. Yang, 2021 Structure detection of horizontal gas–liquid slug flow using ultrasonic transducer and conductance sensor. *IEEE Transactions on Instrumentation and Measurement* **70**: 1–10.
- Zhai, L., B. Xu, H. Xia, and N. Jin, 2023 Simultaneous measurement of velocity profile and liquid film thickness in horizontal gas–liquid slug flow by using ultrasonic doppler method. *Chinese Journal of Chemical Engineering* **58**: 323–340.
- Zhang, H., F. Dong, and C. Tan, 2022 Liquid–solid two-phase flow rate measurement by electrical and ultrasound doppler sensors. *IEEE Transactions on Instrumentation and Measurement* **71**: 1–9.

How to cite this article: Wiranata, L.F., Putra N.K., and Kurniadi D. Detection of Two-Phase Slug Flow Film Thickness by Ultrasonic Reflection *Chaos Theory and Applications*, 6(4), 237-248, 2024.

Licensing Policy: The published articles in CHTA are licensed under a [Creative Commons Attribution-NonCommercial 4.0 International License](https://creativecommons.org/licenses/by-nc/4.0/).

